A study on the usage of Magneto Rheological Elastomers for non-linear aeroelastic oscillations control

Henrique Edno Leoncini de Carvalho[1], Reyolando Manoel Lopes Rebello da Foseca Brasil[1].

[1]*Department of Structural and Geotechnical Engineering, Polytechnic School of the University of São Paulo. Av. Prof. Almeida Prado, trav.2 nº. 83 Edifício Paula Souza (Prédio da Engenharia Civil - Cidade Universitária), 05508-070, São Paulo-SP, Brasil.*

Abstract. Magneto Rheological Elastomers (MRE) are composite intelligent materials, which can substantially change their viscoelastic properties due to their high magneto-sensitivity in response to different regimes of external magnetic field. Under the influence of a magnetic field, both storage shear and loss factor of MREs increase, this field-induced phenomenon is referred to as the magnetorheological effect. The application of MR materials demonstrates great potential for several areas, as indicates the increasing number of patents registered in the last decade. This research is included in a line aimed to develop MRE devices for structural vibrations' control, exploring the magnetorheological effect and its capacity to promote gains in viscoelastic properties, thus enabling changes of relevant magnitudes in structural systems, such as the natural frequency and damping ratio. This adaptive behavior can be studied by the analysis of qualitative numerical simulations, this study proposes to investigate the effectiveness of MRE devices on wind induced aeroelastic oscillations (galloping equation), the results are obtained by the Multiple Scale Method and numerical integrations, showing a trajectory suppression on the phase-plane of limit cycles to focal points, as well as a three-fold change in the critical speed and alterations on the shape of the Hopf's bifurcation diagram.

Keywords: Magneto Rheological Elastomers, aeroelastic, simulation, vibrations, control.

1 Introduction

EMRs are composite materials composed of a solid elastomeric matrix and a dispersion of magnetizable particles such as silicone rubber and carbonyl iron, respectively [1].

The development of numerical simulations that validate the use of EMR materials in vibration control devices in structures is essential for the development of innovative technologies, and is a developing area rich in opportunities.

Within the scope of numerical simulations with EMR dampers, research explores their application in several situations: from the control of seismic effects to the development of finite element models for application in spatial structures [2–4]

1.1 The Magento Rheological Effect

Research on similar Magnetorheological (MR) materials spans approximately seven decades [5]. Composites manufactured with a fluid matrix and magnetizable particles present lower crosslinking density, which allows the movement of the charge in an external magnetic field, forming columnar structures aligned with the equipotentials of an applied external magnetic field, as seen in Figure 1 [6], which illustrates the magnetorheological effect, defined by the tendency of these particles to align, causing changes in the samples the intrinsic viscoelastic properties, increasing both storage and loss modulus.

1.2 Dynamic characterization

Regarding sample characterization, it is necessary to adopt a mathematical physical model to obtain viscoelastic parameters (viscosity and shear modulus). Carvalho (2023) [7] obtained results with a margin of error of

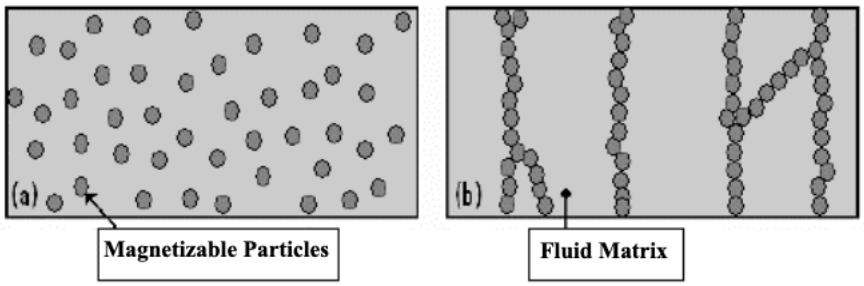

Figure 1. Alignment of magnetizable particles in MR fluids. (a) Null field. (b) Applied external field

3.19%, using the Kelvin Voigt model, pointing out that the dynamic behavior of EMR materials is dependent on the sampling frequency, applied magnetic field and controlled input parameters (displacement amplitude or force). Particularly, for each stress-strain regime to which the material is subjected, a different response is obtained, the different responses translate into adjusted equations for interpolation of results within the established acquisition limits (Equation 1 and Equation 2), with magnetic charge concentration of 33% by volume, sampling frequency f from 10 Hz to 60 Hz, variable magnetic field B from 0.00 T to 0.35 T, and controlled stress T from 1.05 kPa to 5.25 kPa.

$$\begin{aligned}&\eta(f,B,\tau) = \\ &(0.2381\,T - 1.25)\,(3673.0\,B^5 - 36.65\,B^4\,f - 1511.0\,B^4 + 0.2424\,B^3\,f^2 + 5.956\,B^3\,f + 173.1\,B^3 + 0.0004304\,B^2\,f^3 - \\ &0.1869\,B^2\,f^2 + 7.608\,B^2\,f - 113.8\,B^2 - 0.00001659\,B\,f^4 + 0.002739\,B\,f^3 - 0.147\,B\,f^2 + 3.247\,B\,f - 28.57\,B + 7.409\,10^{-8}\,f^5 \\ &- 0.00001436\,f^4 + 0.001073\,f^3 - 0.03916\,f^2 + 0.7284\,f - 6.59) + (0.2381\,T - 0.25)\,(-4162.0\,B^5 - 1.329\,B^4\,f + 3764.0\,B^4 \\ &+ 0.006145\,B^3\,f^2 + 1.494\,B^3\,f - 1239.0\,B^3 - 0.00007538\,B^2\,f^3 + 0.01145\,B^2\,f^2 - 1.346\,B^2\,f + 196.9\,B^2 + 3.451\,10^{-6}\,B\,f^4 \\ &- 0.0006253\,Bf^3 + 0.04063\,B\,f^2 - 1.082\,B\,f + 4.215\,B - 2.46\,10^{-8}\,f^5 + 4.711\,10^{-6}\,f^4 - 0.0003526\,f^3 + 0.01322\,f^2 \\ &- 0.2678\,f + 3.01)\end{aligned} \tag{1}$$

$$\begin{aligned}&G_x(f,B,\tau) = \\ &(0.2381\,T - 0.25)\,(-1943.0\,B^5 + 0.3606\,B^4\,f + 1716.0\,B^4 - 0.001559\,B^3\,f^2 - 0.2479\,B^3\,f - 529.2\,B^3 + 0.00001139\,B^2\,f^3 \\ &- 0.0001621\,B^2\,f^2 + 0.06408B^2\,f + 72.87\,B^2 + 1.119\,10^{-7}\,B\,f^4 - 0.00001031\,B\,f^3 - 0.0001565\,B\,f^2 + 0.02358\,B\,f - 2.437\,B \\ &+ 1.132\,10^{-9}\,f^5 - 2.473\,10^{-7}\,f^4 + 0.00002014\,f^3 - 0.0007694\,f^2 + 0.01439\,f + 0.3403) - 1.0\,(0.2381\,T - 1.25)\,(6286.0\,B^5 \\ &+ 0.7622\,B^4\,f - 5734.0\,B^4 - 0.003087\,B^3\,f^2 + 0.1748\,B^3\,f + 1731.0\,B^3 + 0.0001991\,B^2\,f^3 - 0.02385\,B^2\,f^2 + 0.8044\,B^2\,f \\ &- 191.8\,B^2 - 2.28\,10^{-6}\,B\,f^4 + 0.0003249\,B\,f^3 - 0.01584\,B\,f^2 + 0.3137\,B\,f + 6.276\,B + 9.245\,10^{-9}\,f^5 - 1.49\,10^{-6}\,f^4 \\ &+ 0.00008792\,f^3 - 0.002361\,f^2 + 0.03147\,f + 0.5171)\end{aligned} \tag{2}$$

Where viscosity η is given in kPa.s, and shear modulus G is given in MPa.

1.3 Single Degree of Freedom aeroelastic oscillations

Many structures can be modeled as single-degree-of-freedom systems, which is why it is a recurring case study, serving as a basis for understanding more complex systems. Figure 2 illustrates the case study of this research, while equation Equation 3 describes the free motion of the aeroelastic oscillator.

$$m\ddot{y} + c\dot{y} + ky = \frac{1}{2}\rho V^2 HL[A_1(\frac{\dot{y}}{V}) - A_3(\frac{\dot{y}}{V})^3 + \ A_5(\frac{\dot{y}}{V})^5 - A_7(\frac{\dot{y}}{V})^7] \tag{3}$$

Where mass m is given in kg, stiffness k in N/m, displacement y in meters, damping c in N.s/m, air density $\rho = 1.2kg/m$, prism height H, and width L in meters, incidence velocity V in m/s, constants $A_1 = 2.69$, $A_3 = 168$, $A_5 = 6270$, $A_3 = 59900$, obtained experimentally by Parkinsson (1964) [8], where H=L.

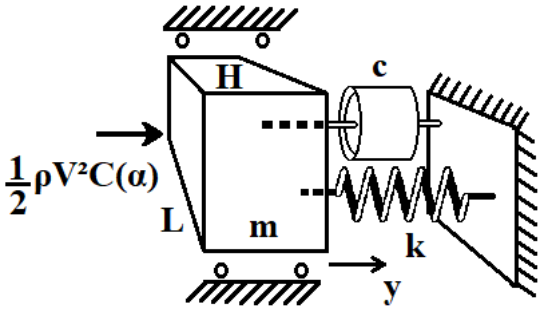

Figure 2. Prismatic mass-spring-damper system, with non-linear input and response

1.4 Aeroelastic gallop of blunt structures

Galloping is defined by oscillations transverse to the wind direction, a phenomenon governed by both the nature (wind direction and intensity) and the geometry of the body.

Cable-stayed bridge cables are common cases of galloping, which, due to their cylindrical shape, promote the shedding of Karman vortices. In 2002, in China, the first known application of a magnetorheological device (liquid matrix) to reduce these effects was dated, making the *Donting Lake* bridge (Figure 3) a reference for the use of this technology [9, 10].

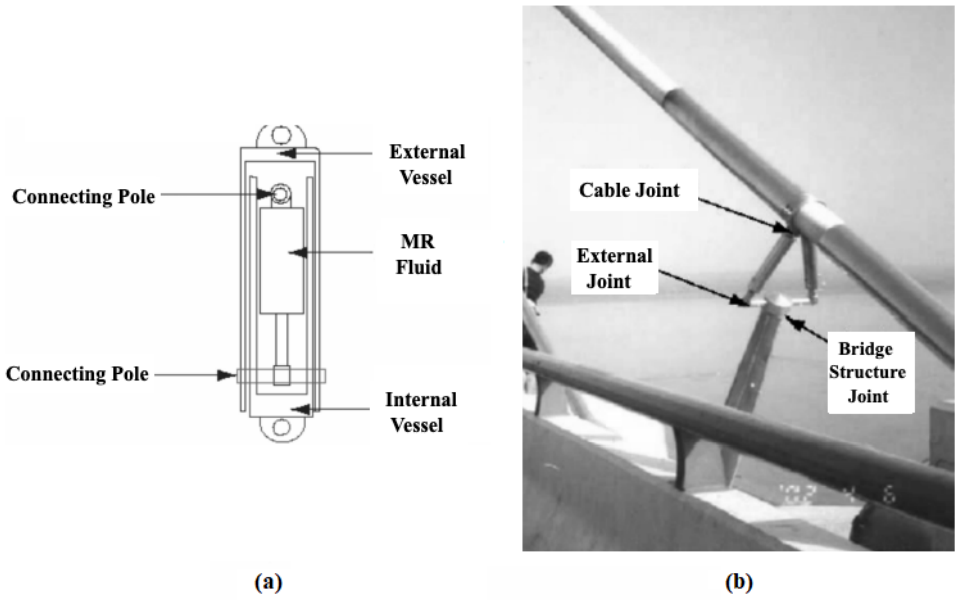

Figure 3. Magnetorheological damping device of *Donting Lake* bridge

2 Methodology

2.1 Stiffness and damping

The experimental data implemented originate from the Kelvin Voigt viscoelastic solids characterization model. For the simplified case of a single-degree-of-freedom oscillator where the deformation is expressed by the ratio between displacement and sample thickness, the damping and stiffness values resemble the linear viscous damping model, expressed by Equation 4:

$$k = \frac{GA}{e} \quad , \quad c = \frac{\eta A}{e} \tag{4}$$

Where $A = 0.01$ is the area of the EMR damper in m², $e = 0.01$ its thickness in meters, considering a double layer sample (10cm x 10cm x 1cm).

2.2 Analytical equations

The gallop equation is rewritten in its dimensionless form by means of algebraic substitutions [11]:

$$\ddot{Y} + Y = nA_1[(U - \frac{2\zeta}{nA_1})\dot{Y} - (\frac{A_3}{A_1U^3}\dot{Y}^3 + (\frac{A_5}{A_1U^5})\dot{Y}^5 - \frac{A_7}{A_1U^7})\dot{Y}^7] \tag{5}$$

$$Y = \frac{y}{h}\ ,\ \tau = \omega t\ ,\ U = \frac{V}{\omega h}\ \ ,\ n = \frac{\rho h^2}{2m}\ ,\ \omega = \sqrt{\frac{k}{m}}\ ,\ \zeta = \frac{c}{2\omega ml} \tag{6}$$

Applying the Multiple Scale Method, one obtains the amplitude equation of the system [12]:

$$\frac{\mathrm{d}R(\phi)}{\mathrm{d}\phi} = \frac{1}{2}\varepsilon[(UA_1 - \frac{2\zeta}{n})R - \frac{3}{4}\frac{A_3}{U}R^3 + \frac{5}{8}\frac{A_5}{U^3}R^5 - \frac{35}{64}\frac{A_7}{U^5}R^7] \tag{7}$$

The critical speed Vc (m/s) of this system is obtained by linearizing Equation 3, considering very small oscillations, and defines the first bifurcation point in the stable regime.

$$V_C = \frac{2c}{\rho hlA_1} \tag{8}$$

A qualitative analysis is proposed, since the acquisition limits of the available data are not comprehensive. The simulated system is arbitrary, with mass $m = 45$, and fixed at tension $\tau = 1.05kPa$, frequency $f = 30hz$, with variable field from zero to maximum ($B = 0.35T$).

3 Results and Discussion

Analyzing the Hopf's bifurcation diagram of the nonlinear system, an almost three-fold increase in the critical speed is observed, and consequently, also in the limit cycles (Figure 4). Two points of interest were highlighted (points 0 and 1), which correspond to the maximum amplitude in the original condition of the system that, when the magnetic field is activated, changes its periodic solution to a focal point, suppressing the trajectory.

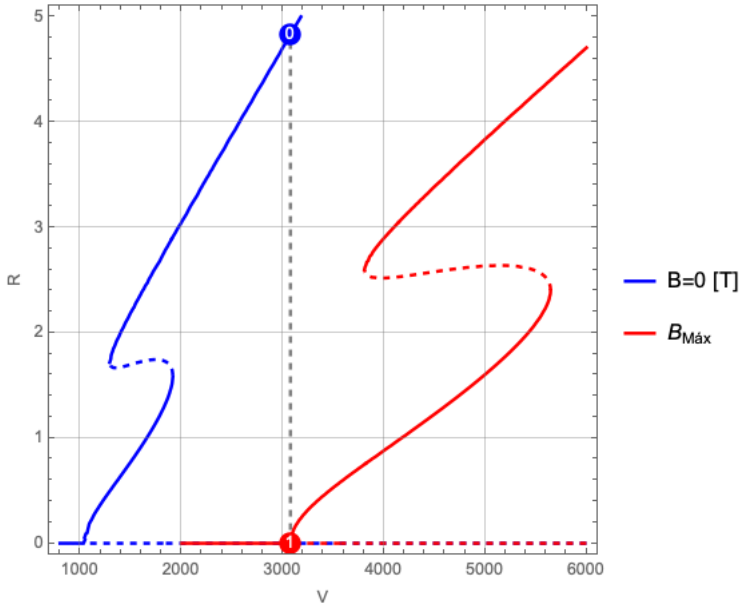

Figure 4. Hopf's bifurcation diagram (amplitude E, velocity V).

The plot of the phase portraits reveals changes in the trajectory curves at the points of interest, within stable regimes (Figure 5).

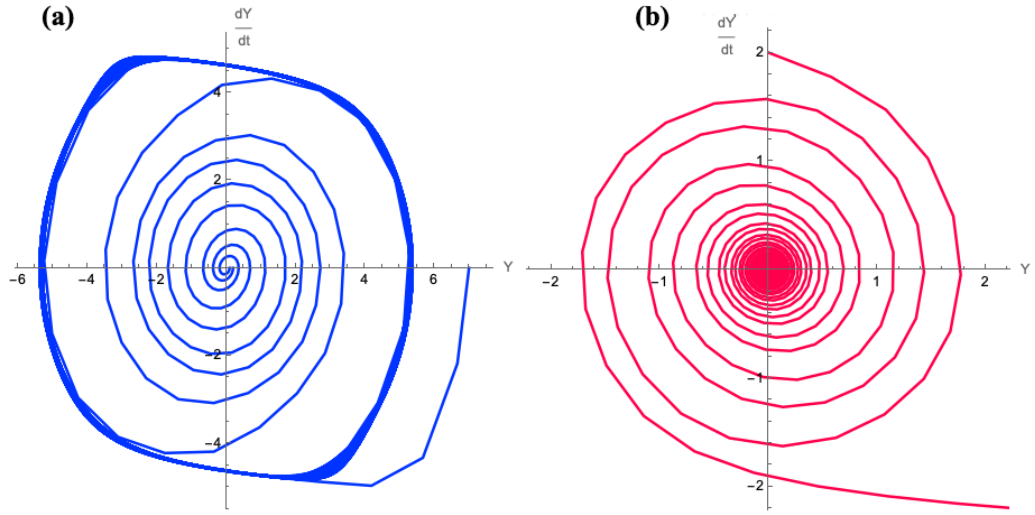

Figure 5. Phase portraits. (a) Point 0. (b) Point 1.

The displacement response (Figure 6) highlights the transition between periodic and damped motion, with great action provided by active damping.

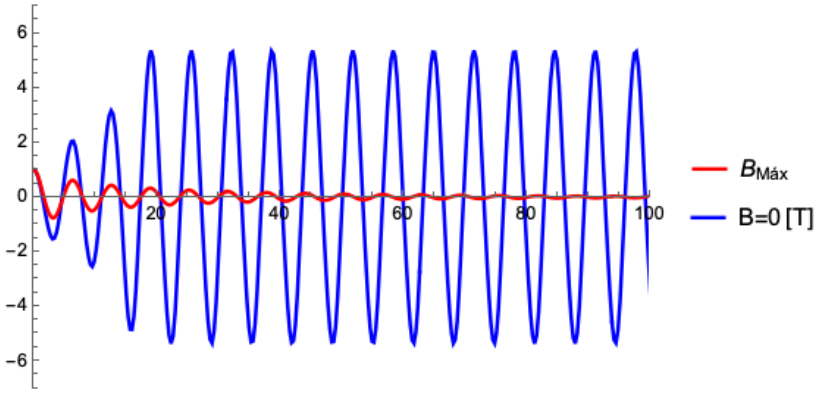

Figure 6. Displacement response in zero and maximum applied external field.

4 Conclusions

Through simulations in an arbitrary system, the great potential for the development of control technologies for systems based on the use of EMR materials was verified, with great effectiveness in changing the behavior of a nonlinear system, also demonstrating the sensitivity of these systems to variable viscoelastic parameters. The activation of the external magnetic field was able to drive the trajectory of the movement from periodic limit cycles to a damped decaying spiral movement, as well as an increase in the critical speed by about three times its value in a null field. The change in the shape of the Hopf bifurcation diagram was also observed, with visible ”stretching” also indicating the effect of the increase in active stiffness.

Acknowledgements. This study was financed in part by the Coordenação de Aperfeiçoamento de Pessoal de Nível Superior – Brasil (CAPES) – Finance Code 001.

Authorship statement. : The authors hereby confirm that they are the sole liable persons responsible for the authorship of this work, and that all material that has been herein included as part of the present paper is either the property (and authorship) of the authors, or has the permission of the owners to be included here.

References

[1] Y. Xu, X. Gong, S. Xuan, W. Zhang, and Y. Fan. A high-performance magnetorheological material: preparation, characterization and magnetic-mechanic coupling properties. *Soft Matter*, vol. 7, n. 11, pp. 5246–5254, 2011.

[2] F. C. d. Almeida. Vibrations isolation in bridge structures using magnetorheological elastomer. Master's thesis, Universidade Estadual Paulista UNESP, Ilha Solteira, São Paulo, Brazil, 2021.

[3] B. X. Jia, F. Gao, and W. F. Bian. Vibration control of space truss structure with viscoelastic laminated composite damper. In *Advanced Materials Research*, volume 971, pp. 860–863. Trans Tech Publ, 2014.

[4] M. Mehrabi, M. Suhatril, Z. Ibrahim, S. Ghodsi, and H. Khatibi. Modeling of a viscoelastic damper and its application in structural control. *PloS one*, vol. 12, n. 6, pp. e0176480, 2017.

[5] J. Rabinow. The magnetic fluid clutch. *Electrical Engineering*, vol. 67, n. 12, pp. 1167–1167, 1948.

[6] P. Skalski and K. Kalita. Role of magnetorheological fluids and elastomers in today's world. *acta mechanica et automatica*, vol. 11, n. 4, pp. 267–274, 2017.

[7] de H. E. L. Carvalho. A study on the usage of magneto rheological elastomers for vibrations control in structures. Master's thesis, Universidade Estadual Paulista UNESP, Ilha Solteira, São Paulo, Brazil, 2023.

[8] G. Parkinson and J. Smith. The square prism as an aeroelastic non-linear oscillator. *The Quarterly Journal of Mechanics and Applied Mathematics*, vol. 17, n. 2, pp. 225–239, 1964.

[9] Z. Chen, X. Wang, J. Ko, Y. Ni, B. F. Spencer Jr, and G. Yang. Mr damping system on dongting lake cable-stayed bridge. In *Smart structures and materials 2003: smart systems and nondestructive evaluation for civil infrastructures*, volume 5057, pp. 229–235. International Society for Optics and Photonics, 2003.

[10] C. M. R. Moutinho. *Vibrations control in civil engineering structures, 2007*. PhD thesis, Faculdade de Engenharia Universidade do Porto FEUP, Porto, Portugal, 2007.

[11] J. M. T. Thompson. *Instabilities and catastrophes in science and engineering*. John Wiley & Sons Ltd., Chichester, New York, Brisbane, Toronto, Singapore, 1982.

[12] M. P. Paidoussis. *Fluid-structure interactions: slender structures and axial flow*, volume 1. Academic press, 1998.